

William Callahan, Bruce B. Hicks*, William R. Pendergrass Jr.**, and Christoph A. Vogel**

AWS Convergence Technologies, Inc
12410 Milestone Center Drive
Germantown, MD 20876

* Metcorps
P.O. Box 1510
Norris, TN 37828

** NOAA/ARL/ATDD
P.O. Box 2456
Oak Ridge, TN 37831

1. INTRODUCTION

In conducting hazard assessments, data from the nearest NWS Automated Surface Observing System weather station are conventionally used as input for dispersion modeling, but these data are generally distant from the location of interest, and provide little information on turbulence. Figure 1 illustrates some of the difficulties that arise. Wind roses generated from data collected using micrometeorological towers erected on rooftops of central Washington, DC, are quite different from that derived from the nearest station of the National Weather Service, at Washington Reagan National Airport.

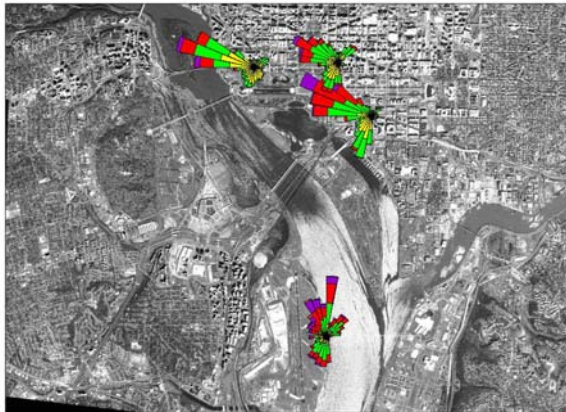


Figure 1. Wind roses derived from three months of hourly data collected at the National Weather Service site at Washington Reagan National Airport and at three DCNet sites in downtown Washington, DC. Data are sorted into wind speed classes, extending out to a maximum of 10 m/s (0 – 1; 1 – 3; 3 – 5; 5 – 7; 7 – 10; starting at the origin).

The focus of the present work is to build upon comparisons between data from a commercial surface network (that of AWS Convergence Technologies, Inc.) and a NOAA urban research

network to show how such commercial surface network data might be used to augment standard dispersion modeling. The AWS “Weatherbug” network uses mechanical anemometers with starting speeds of about 1 m/s, typically deployed on 3 m masts attached at the edges of the roofs of buildings. Research (DCNet) network data are obtained using sonic anemometers mounted 10 m above the roofs of buildings “of convenience,” predominately in the metropolitan area of Washington DC with two additional stations in New York City. The DCNet installations are sited to minimize the consequences of edge effects and local obstructions.

Hicks et al., (2008) have shown that the aggregated data from surface stations surrounding a central rooftop tower are highly correlated with the tower observations. Two potential applications then arise: a) concerning the use of such surface data to predict dispersion within the urban roughness layer, and b) using these same surface data to forecast dispersion across the urban area in question, above the roughness layer. These applications will be addressed here in two different ways. First, methods for extracting the familiar dispersion model inputs from surface network data will be explored. Second, “amplification factors” by which conventional models might be adjusted to account for the effects of enhanced urban roughness will be developed.

Figure 2 shows the stations used in the present analysis, for both Washington DC and New York City (where two additional DCNet stations are located).

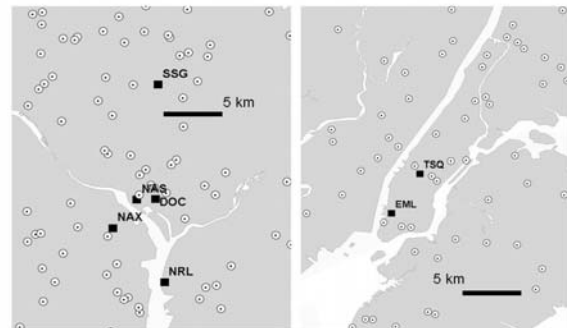


Figure 2. The locations of DCNet and AWS surface sites in the Washington, DC, area (left) and in New York City (right).

Corresponding author address: Bill Callahan, AWS Convergence Technologies, Inc., 12410 Milestone Center Drive, Germantown, MD 29876; e-mail: bcallahan@AWS.com

2. FORECASTING DISPERSION FOR THE SURFACE BOUNDARY LAYER

Puffs of pollutants respond to instantaneous variations in the local wind. Such variations are usually considered as elements of the relevant statistical distributions – $\sigma(u)$ and $\sigma(\theta)$ (or $\sigma(U)$ and $\sigma(V)$) – used to initialize a conventional dispersion model. Here, u is the wind speed, U and V are the east-west and north-south components respectively, and θ is the wind direction. Later, ϕ will be introduced as the vertical plume dimension. The challenge is to derive relevant dispersion statistics for the surface roughness sublayer in which people are exposed. The main quantities of interest are:

For each site of the local subnetwork –

\underline{u} and $\underline{\theta}$: The average wind speed and direction derived over a 15 minute period (or whatever other averaging period might be convenient, in the range 15 to 60 minutes so as to capture all of the turbulent covariance while not strongly violating the desire for stationarity).

$\sigma(u)$ and $\sigma(\theta)$: The standard deviations of the wind speed and wind direction.

\underline{U} and \underline{V} : The average east-west and north-south velocity components derived from wind speed and direction data reported from the same site.

$\sigma(U)$ and $\sigma(V)$: The corresponding standard deviations of the velocity components.

For the subnetwork aggregations from N stations –

$\underline{\underline{U}}$ and $\underline{\underline{V}}$: The subnetwork averages of the \underline{U} and \underline{V} . $\underline{\underline{U}} = (\sum \underline{U})/N$, and similarly for $\underline{\underline{V}}$.

$\sigma(\underline{\underline{U}})$ and $\sigma(\underline{\underline{V}})$: The standard deviations associated with the $\underline{\underline{U}}$ and $\underline{\underline{V}}$ values.

$\underline{\sigma(\underline{U})}$ and $\underline{\sigma(\underline{V})}$: The averages of the N values of $\sigma(U)$ and $\sigma(V)$.

From this set of variables, the goal is to derive the input variables common in plume/puff modeling – the plume transport variables u and θ , and the diffusion factors $\sigma(u)$, $\sigma(\theta)$ and $\sigma(\phi)$.

3. DERIVING u , θ , $\sigma(u)$ & $\sigma(\theta)$ FROM VELOCITY COMPONENT STATISTICS.

Wind Speed. The wind speed (u) to be used in dispersion computations can be derived from (a) a nearby ASOS station, (b) synoptic-scale weather predictions, (c) local meso-scale models, (d) specialized installations like DCNet, or (e) surface network data such as are considered here. Of these choices, the first two appear susceptible to considerable error. The third appears a reasonable

source of wind speed information at the level of skimming flow, from which surface wind speeds can be estimated as about 30% to 40% of the predicted skimming flow speed (Hicks et al., 2008). Figure 3 illustrates the relationship between network averaged wind speed and that observed by the central DCNet tower. The overall agreement is not particularly pleasing. If actual observations are available in real time, then clearly (d) could prove preferable, yielding surface wind speeds typically 30% to 40% of the rooftop mast measurement. However, if the intent is to address dispersion within and through the urban roughness layer, reliance on surface wind measurements would appear preferable, provided that these are aggregated to obtain a best estimate. There is a basic guidance principle that appears relevant – To forecast well, minimize the stretch (in both space and time) from available data. Real-time local data are the best on which to rely, provided they are used appropriately.

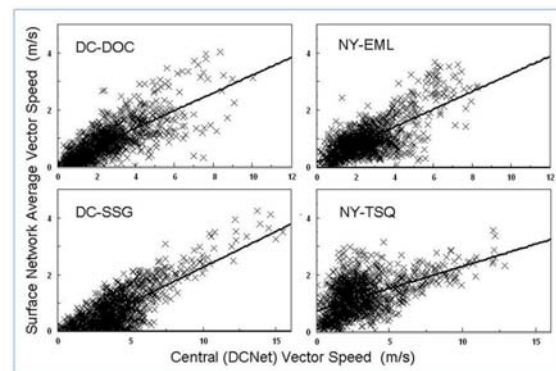


Figure 3. The relationships between AWS-station and DCNet tower wind speeds, for two weeks of October 2006 and for four sites of the DCNet program. The vertical axis plots surface average vector speeds, derived by averaging the velocity components reported by network anemometers over each 15-minute run, and then combining the average velocity components to derive the average network speed.

Wind direction. Although there is limited correlation between the wind speeds aloft and those within the surface roughness sublayer, the wind directions appear to be consistent. This is illustrated in Figure 4. The network average wind direction data are derived from the average velocity components \underline{U} and \underline{V} . As must be expected, low-wind-speed performance limitations of the surface network anemometers impose considerable scatter, and consequently Figure 4 addresses only those cases for which the average surface network wind speed exceeded 1 m/s.

It is concluded that the subnetwork vector mean wind direction is well connected to the wind direction aloft for urban areas with low aspect ratios (i.e. $F_r < 0.5$,

see Baik et al., 2000), and that in such situations either of these would provide a good basis for estimating the direction of drift of puffs dispersing in the surface sublayer. The matter of the influence of street canyon aspect ratio on wind direction “rectification” remains to be explored.

Table 1

Relationships between the average vector speed derived from the surface network within 5 km of the central DCNet site and the DCNet speed. The relationship tested is of the form $Y = a + b.x$, or $Y = B.x$, where Y is the surface average vector speed, and x is the central DCNet speed. R is the correlation coefficient.

| | <u>All Winds</u> | | | <u>Wind > 1 m/s</u> | | |
|--------------------------|------------------|------|------|------------------------|------|------|
| | R | b | B | R | b | B |
| Washington, DC | | | | | | |
| DOC | 0.76 | 0.31 | 0.36 | 0.63 | 0.24 | 0.40 |
| NAS | 0.80 | 0.36 | 0.42 | 0.67 | 0.23 | 0.48 |
| NAX | 0.82 | 0.18 | 0.18 | 0.66 | 0.13 | 0.20 |
| NRL | 0.87 | 0.29 | 0.28 | 0.85 | 0.29 | 0.24 |
| SSG | 0.75 | 0.25 | 0.18 | 0.84 | 0.23 | 0.27 |
| New York City, NY | | | | | | |
| EML | 0.71 | 0.31 | 0.38 | 0.66 | 0.29 | 0.40 |
| TSQ | 0.51 | 0.16 | 0.41 | 0.54 | 0.16 | 0.39 |

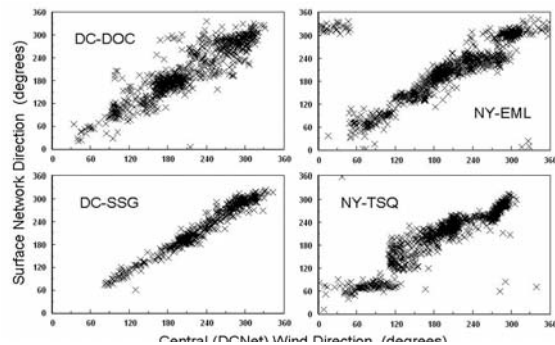


Figure 4. As in Figure 3, but comparing average wind directions on a 15-minute vector-resolved basis. To avoid light wind sensor limitations, data are confined to average network wind speeds above 1 m/s. Note the evidence of street canyon “rectification” of the wind field for the New York City data, especially for the TSQ observations.

Wind Speed Standard Deviation. The focus so far has been on combining the data from separate origins, using the orthogonal velocity components U and V . Continuing in this mode, it is of relevance to consider how $\sigma(u)$ relates to $\sigma(U)$ and $\sigma(V)$. Deriving $\sigma(u)$ from quantifications of $\sigma(U)$ and $\sigma(V)$ given by a single anemometer requires estimation of the covariance between the U and V components, normally accomplished by coordinate rotation. The validity of the extension of this to a network is not obvious. Certainly, the vector speed standard deviation defined by

$$\sigma(\text{speed}) = \sqrt{(\sigma(U)^2 + \sigma(V)^2)} \quad (1)$$

provides an approximation. Figure 5 illustrates the relationship between $\sigma(\text{speed})$ as defined above and the value $\sigma(u)$ obtained by formal coordinate rotation, for 15 minute groupings of 10 Hz observations from the four DCNet sites. These plots use a complete year of data from each site. In all cases, the slopes are exceedingly close to unity, with individual values as shown, so that a proportionality between $\sigma(\text{speed})$ and $\sigma(u)$ is supported on the average. The average slope (i.e. the power law exponent) derived from all of the sites is 1.02 ± 0.01 , so that the expected linear relationship is clearly supported by the data. The constant of proportionality based on all sites listed in Table 1 is $0.74 (\pm 0.01)$. The overall correlation coefficient is 0.97 . As elsewhere in the present treatment, it is tacitly assumed that the constant of proportionality (0.74) also applies to the aggregation of wind components across a local network. This is certainly debatable, since the covariances of the contributing north-south and east-west components across the subnetwork need to be considered, and those are not readily derived from the present data.

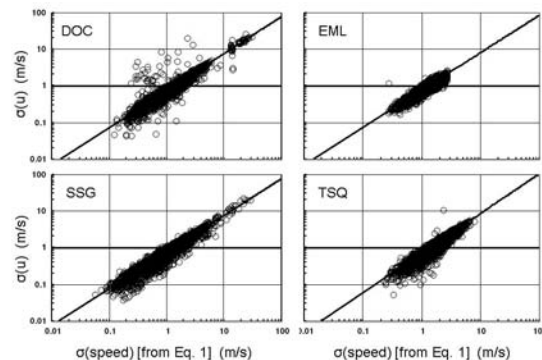


Figure 5. The relationships between two different measures of the longitudinal wind speed standard deviation – $\sigma(u)$ as derived by full coordinate rotation of velocity components from three-dimensional anemometers, and the approximation $\sigma(\text{speed})$ derived as in Equation 1. In all cases, the (power law) regression lines indicate that proportionality is a good approximation.

Wind Direction Standard Deviation, $\sigma(\theta)$. There is need to derive appropriate values of $\sigma(\theta)$ from values of the average velocity components and standard deviations. Turner (1986) reviews three alternative methods, but all require the acquisition of statistical quantities not easily obtained for the surface network considered here. Given that for the present network application it is preferred to make use of the orthogonal velocity components, Equation 2 appears to provide an appropriately straightforward (although imprecise) answer:

$$\sigma(\theta) \sim \text{Arctan}[(\sigma(U) + \sigma(V))/(2(U^2 + V^2))^{1/2}] \quad (2)$$

This can be tested with DCNet data, since the instrumentation and data acquisition systems of the DCNet program permit turbulence quantities to be recorded in several different ways. In particular, time averages of the wind speed and $\sigma(\theta)$ are computed directly and recorded every fifteen minutes. In parallel, the wind vector component averages and standard deviations are computed and recorded – \underline{U} and \underline{V} , and $\sigma(U)$ and $\sigma(V)$. Figure 6 compares predictions made using Equation 2 with direct measurements of $\sigma(\theta)$, for the four sites considered here – DOC, SSG, EML and TSQ. The similarities among the diagrams of Figure 6 are striking, with the overall conclusion that the simple relationship (2) yields estimates of $\sigma(\theta)$ about 10% below the direct measurements, except for very high values (above about 70 degrees).

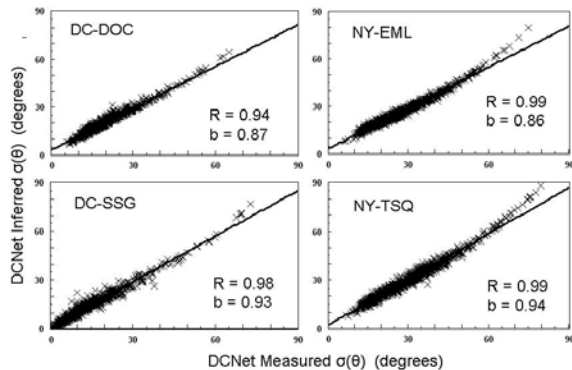


Figure 6. Tests of Equation (2), for extracting $\sigma(\theta)$ values from aggregated velocity component data. DCNet data are used. Results obtained using Equation (2) are plotted against actual direct measurements of $\sigma(\theta)$ derived from sonic anemometry. Linear regression lines are shown, with correlation coefficients R and slopes b.

Diffusion in the Vertical, $\sigma(\phi)$. Within the data sets provided by surface networks, there appear to be no direct measurements that would lead to immediate quantification of $\sigma(\phi)$. In practice, the role of street canyons will be a key consideration. However, Figure 7 provides a possible opportunity – inspection of the diagram reveals that the relationship between $\sigma(w)$

and $\sigma(v)$ is much the same for all of the sites: $\sigma(w) \approx 0.65\sigma(v)$. Using this result as a starting point, it is apparent that a first estimate of $\sigma(\phi)$ can be obtained by applying this same constant of proportionality, so that $\sigma(\phi) \approx 0.65\sigma(\theta)$.

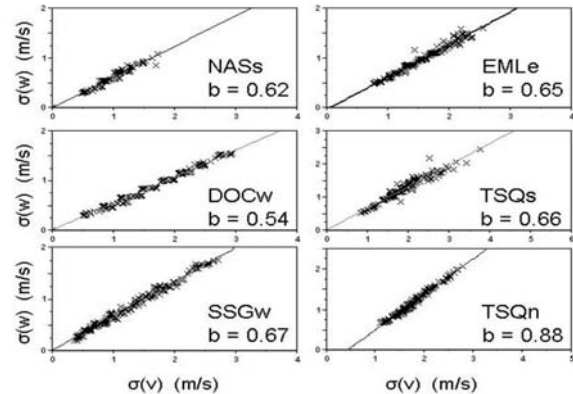


Figure 7. Using coordinate-rotated DCNet sonic anemometer data alone, sample plots of the vertical wind component standard deviation against the transverse. The identifiers n, e, w, and s indicate the wind directions from which the data are selected – north, east, etc. Slopes are given as “b.”

4. APPLYING THE RESULTS.

There are two obvious ways in which surface network data might be used in modified plume dispersion models: (a) by applying “amplification factors” to the results of conventional models that are driven by descriptions of u , θ , $\sigma(u)$ and $\sigma(\theta)$ based on some methodology developed for application in simpler circumstances (e.g. the Pasquill-Gifford categorization approach), or (b) by employing a dispersion code that makes use of observed values of the average wind and its turbulence (i.e. u , θ , $\sigma(u)$, $\sigma(\theta)$ and $\sigma(\phi)$). In both cases, a first step is to aggregate wind vector components provided by the anemometers in a subnetwork within some specified radius of the location of principal interest -- the release point of some trace gas for example.

Dispersion amplification factors. Figure 8 presents plots of two ratios of potential utility in adapting standard models to an urban environment like that studied here. The first is the ratio (F_1) of (a) the value of $\sigma(\theta)$ derived from the averages \underline{U} , \underline{V} , and the corresponding standard deviations using Equation (1), to (b) the value of $\sigma(\theta)$ derived similarly from the U and V component statistics from the central DCNet tower. The intent is to quantify a factor that could be used to address a suburban setting if skimming-flow or near-surface tower data are all that are available. The second is the ratio (F_2) of the $\sigma(\theta)$ value derived from the mean wind vectors reported by the independent surface stations to the $\sigma(\theta)$ value derived from the averages of the standard deviations (in time)

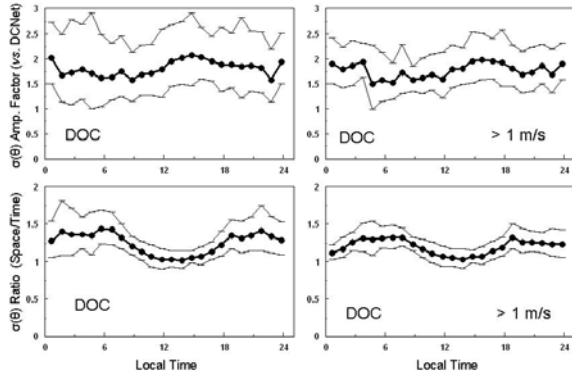


Figure 8. Two characterizations of the behavior of $\sigma(\theta)$ at the surface. At the top are ratios of $\sigma(\theta)$ derived from the surface array surrounding the DOC central DCNet site to the value of $\sigma(\theta)$ derived from the average U and V components measured by the DCNet instrumentation. Below are values of the space to time ratios for $\sigma(\theta)$, based on the surface array alone. The diagrams at the right are constrained to surface average wind speeds above 1 m/s.

reported by the same stations. F_2 is the ratio space/time of the surface $\sigma(\theta)$ field. Figure 8 is for the DOC location. Figure 9 is the corresponding diagram for New York City. All other sites yield similar behavior, with the evidence of light-wind sensor limitations being strongly evident for the nighttime hours, and with the data being more orderly when cases with average wind speeds below 1 m/s are excluded. In many of the cases there is some residual evidence of a diurnal cycle, but the amplitude is small enough that it is disregarded at this time.

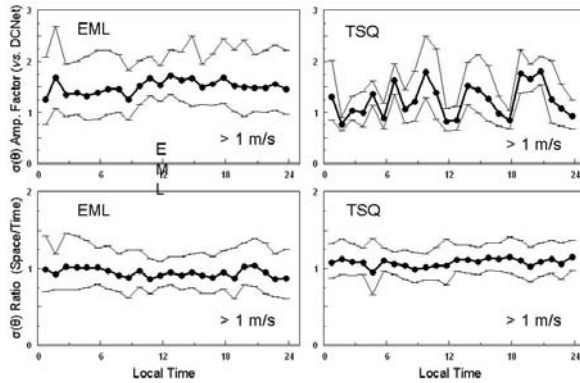


Figure 9. An extension into New York City, for two DCNet sites and the surface subnetwork surrounding them (within 5 km) – EML near the Houston Street subway station and TSQ near Times Square. Only cases with average surface wind speeds exceeding 1 m/s are used in the analysis.

Table 2 lists the values of the factors F_1 and F_2 characterizing a number of subnetworks, including the New York City cases. The values of F_1 vary considerably, especially for the all-winds case. This variability is reduced substantially when the data are constrained to speeds above 1 m/s. There is no basis for expecting the F_1 values listed for the higher-speed cases to be different for light winds, but there is also no way in which this can be tested using the present data set. It should also be noted that the values of F_1 are universally greater than unity, implying that the turbulence levels detected by the surface network are greater than those of the higher-altitude DCNet. However, it should be remembered that the present amplification factors apply to cross-wind variability only. It was shown earlier (Hicks et al., 2008) that the statistics of the wind components themselves indicate a near-equality between the turbulence intensities aloft and those deduced from the surface network. There is no significant distinction between the space/time ratios for any of the sites summarized in the table.

Table 2

Summaries of the ratios describing the relationships between surface values of $\sigma(\theta)$ and values measured by the central DCNet towers at the locations indicated (see Table 1). F_1 is the ratio of $\sigma(\theta)_{\text{time}}$ to $\sigma(\theta)_{\text{DCNet}}$. F_2 is the ratio $\sigma(\theta)_{\text{space}}/\sigma(\theta)_{\text{time}}$ for the surface subnetwork data set. Two values are listed for each variable, F_1 and F_2 , one value computed using all data, the other with wind speeds constrained to > 1 m/s. The values in parentheses are standard deviations. Since the means are computed geometrically, the standard deviations should be interpreted as \times/\div rather than the conventional $+/-$.

| | F_1 | | F_2 | |
|-----|----------------|----------------|----------------|----------------|
| | All u | > 1 m/s | All u | > 1 m/s |
| DOC | 1.81 (1.43) | 1.78 (1.29) | 1.24 (1.22) | 1.18 (1.15) |
| NAS | 1.69 (1.50) | 1.57 (1.31) | 1.26 (1.23) | 1.19 (1.17) |
| NAX | 2.14 (1.48) | 2.24 (1.23) | 1.38 (1.28) | 1.19 (1.09) |
| SSG | 3.11 (1.79) | 2.22 (1.26) | 1.03 (1.49) | 0.77 (1.18) |
| EML | 1.45 (1.46) | 1.52 (1.46) | 0.97 (0.98) | 0.93 (1.33) |
| TSQ | 1.13 (1.54) | 1.20 (1.51) | 1.11 (1.26) | 1.09 (1.22) |

Direct Computation. The second potential path to follow is to make use of aggregated data from the available surface stations to drive dispersion calculations directly. Instead of estimating the properties u , θ , $\sigma(u)$, $\sigma(\theta)$ and $\sigma(\varphi)$ from external sources, derive values appropriate for the area of interest using the methodologies outlined above, based on consideration of all surface stations in the vicinity of the origin of relevance. What constitutes the appropriate “vicinity” remains to be fully explored. Here, a radius of 5 km has been used, on purely heuristic grounds. Selection of surface stations to be used in such aggregation will require local knowledge, especially in terrain more complex than that considered here.

In either approach, it is accepted that at some downwind distance the diffusing material will become integrated with the skimming flow aloft, at which time the more conventional regional-scale dispersion approaches will become more relevant. At this time, it is not clear where this “handover” might occur, but guidance from a number of sources leads to the suspicion that it will be at a distance in the range 2 to 10 km, depending on the characteristics of the area. The present purpose is not to propose answers to all relevant questions of this kind, but to suggest a path that might profitably make use of local network data.

5. CONCLUSIONS

Examination of wind roses derived using data collected in the central business district of Washington, DC, with wind roses derived from the nearby airport show that in this case the airport data are not indicative of flow affecting the downtown area.

The wind speeds yielded by combining data from a local network of roof-edge anemometers are well correlated with the measurements at DCNet stations located 10 m above rooftops, although not as well correlated as for the velocity standard deviations. The average ratio of surface mean wind speed to DCNet rooftop speed is about 0.3 for the Washington situations considered here, and 0.4 for the two New York stations. Early studies in the suburbs of Chicago yielded similar results (Fujita and Wakimoto, 1982), and Hanna et al. (2006) have reinforced this finding using more recent observations.

Provided the individual network sensor systems yield accurate wind field information, relatively simple techniques can be used to approximate the conventional plume dispersion quantities $\sigma(u)$ and $\sigma(\theta)$ from data aggregated from many surface stations. The results can then be employed in a variety of ways, either by modifying conventional dispersion codes or by making use of the observations themselves to drive the dispersion routines. The details of this transformation remain to be fully explored for network situations. In any case, the methodologies proposed here appear more

appropriate for suburban rather than city-center applications, because observations of tracer movement in high aspect ratio city street canyons indicate that the material moves as puffs that retain considerable integrity. Hence, the smoothed statistical descriptions provided by standard models appear inappropriate.

Alternatively, it is feasible to employ local surface network data to derive the key quantities required to initialize dispersion routines. The number of stations necessary to compile meaningful averages of the important variables remains poorly determined, but the evidence available for the cities addressed here (Washington DC, and New York City) indicates that ten stations could be adequate. The density of locations in these two cities is such that this corresponds to an area with a radius of about 5 km around a location of specific interest. If the amplification factor approach is used, then it is necessary to assume that the surface is homogeneous across this spatial domain. Such an assumption is also inherent in the reliance on the derivative data themselves -- these data will certainly carry with them the signatures of any spatial inhomogeneities that might exist. In other words, caution is recommended before extrapolating the present results to an area that has more terrain complexity than the two situations considered here.

The matter of dispersion in the vertical direction requires special consideration. Tracer studies conducted in New York City suggest that the street canyons are filled as puffs migrate according to the local wind. In the lack of contrary evidence, it is tentatively concluded that the matter of vertical turbulence and diffusion might be approximated using the same amplification factors as are developed here for the cross-wind case. It is acknowledged that the methodologies developed here will result in nowcasts rather than genuine forecasts. The persistence of these nowcasts has been addressed elsewhere (Vogel and Pendergrass, 2007). For the present, it should be noted that a cardinal time scale will be determined by the radius of the area across which surface station data are used and the velocity affecting the dispersion in the surface roughness layer – for the present implying a characteristic time scale of about $5/U$ hours, where U is the skimming flow wind speed in m/s. Vogel and Pendergrass conclude that surface data of the kind reported here yield critical lag times in the range one to three hours, with an average of about 2.2 hours, suggesting that persistence would be a good way to proceed given the availability of local meteorological data updated every 15 minutes.

ACKNOWLEDGEMENTS.

Several staff members of the NOAA Air Resources Laboratory assisted with the analyses presented here, especially Ron Dobosy and Ed Dumas of Oak Ridge,

and Roland Draxler of Silver Spring. Continuing Congressional interest in the program is greatly appreciated. The present reliance on data from AWS Convergence Technologies, Inc., should not be construed as an endorsement of this company by NOAA or its employees.

REFERENCES

Baik, J-J., R-S Park, H-Y. Chun, and J-J. Kim, 2000: A Laboratory Model of Urban Street-Canyon Flows. *J. Appl. Meteorol.*, **39**, 1592 – 1600.

DePaul, F. T. and C-M. Sheih, 1985: A Tracer Study of Dispersion in an Urban Street Canyon. *Atmos. Environ.*, **19**, 555 – 559.

DePaul, F. T. and C-M. Sheih, 1986: Measurements of Wind Velocities in a Street Canyon. *Atmos. Environ.*, **20**, 455 - 459.

Fujita, T. T. and R. M. Wakimoto, 1982: Effects of miso- and mesoscale obstructions on PAM winds obtained during project NIMROD. *J. Appl. Meteorol.*, **21**, 840 – 858.

Hanna, S. R., J. White, Y. Zhou and A. Kosheleva, 2006. Analysis of Joint Urban 2003 (JU2003) and Madison Square Garden 2005 (MSG05) Meteorological and Tracer Data. Paper J7.1 of the Sixth AMS Conference on the Urban Environment, Atlanta, GA, available at http://ams.confex.com/ams/Annual2006/techprogram/paper_104131.htm.

Hicks, B. B., W. R. Pendergrass, C. A. Vogel, and R. S. Artz, 2008; On the coupling between urban surface wind fields and skimming flow. Paper J16.1, this conference.

Turner, D. B., 1986: Comparison of three methods for calculating the standard deviation of the wind direction. *J. Climate and Appl. Meteorol.*, **25**, 703 - 707.

Vogel, C. A., and W. R. Pendergrass, 2007. Using autocorrelation to evaluate persistence forecasts for discrete wind vector fields in the National Capital Region. Paper P1.15 of the American Meteorological Society 2007 Annual Meeting, available at <http://ams.confex.com/ams/pdfpapers/127139.pdf>.